ELSEVIER

Sensors and Actuators A 103 (2003) 48–58

SENSORS AND ACTUATORS A PHYSICAL

www.elsevier.com/locate/sna

A reliable single-layer out-of-plane micromachined thermal actuator☆

Wen-Chih Chen, Chien-Cheng Chu, Jerwei Hsieh, Weileun Fang*

Power Mechanical Engineering Department, National Tsing Hua University, Hsinchu, Taiwan, ROC

Abstract

Out-of-plane electrothermal actuators have been applied to a variety of fields with the bimorph effect being the most commonly used driving method, due to simple fabrication process. However, such an actuator experiences a shear force at the interface of different materials, while actuated. Delamination therefore takes place and decreases its lifetime. In this study, a novel bi-directional out-of-plane electrothermal actuator is designed and fabricated. Unlike the bi-metal and hot–cold arm thermal actuator, this actuator can move in two directions. Since this actuator is consisted of only single-layer thin film material, it can prevent from delamination. According to the static load–deflection test, this actuator can achieve bi-directional actuation with amplitude near 6–7 μm when driven at 5 V. According to the vibration test, the dynamics of the actuator is influenced not only by the thermal characteristics but also by the vibration modes. Consequently, the thermal actuator still has a significant output when driven near 40 kHz. The actuator were experienced a fatigue test which shows that its resonant frequency remains unchanged after 10^9 cycles of continuous operation with driving voltage at 2.25 V.

Keywords: Thermal actuator; Delamination; Bulk micromachining; Fatigue test

1. Introduction

Microactuator is one of the key components for MEMS devices. According to the motion of the actuators, they can be categorized as in-plane actuator [1–3] and out-of-plane actuator [4–6]. The out-of-plane actuators can convert input signals into displacement normal to the surface of a silicon wafer. They accordingly have many applications, for instance the optical scanner [7], optical switch [8], micro-relay [9], variable capacitor [10], and so on. There are various approaches, such as magnetic, electrostatic, electro-thermal, and piezoelectric, have been employed to drive the out-of-plane actuators. The electrothermal actuators have the advantages of low operation voltage, simple fabrication process and CMOS-compatible. They have been exploited to drive various MEMS devices [11–13]. In this study, the electrothermal out-of-plane actuator is discussed.

The existing out-of-plane thermal actuators are usually multi-layer structures. For instance, the bi-layer electrothermal actuator employed the bimorph effect to generate out-of-plane motion. Such a bi-layer actuator comprises two materials which coefficients of thermal expansion differ from each other. The application of a temperature-change stimulus would thus give rise to out-of-plane displacement since the expansions of both layers are different [14]. As a second example, Bright and co-workers [15] presented a multi-layer electrothermal actuator consisted of only a single material. The actuator comprised a few beams of different cross-sectional areas. While a current is applied, different deflection of beams accompanying temperature rise caused out-of-plane motion. However, these multi-layer actuators experience a shear force at the interface of different layers, while actuated. Delamination consequently would take place after a long-term operation and consequently decreases its lifetime. In addition, these actuators can only bend in one direction while heating.

To fabricate electrothermal actuator using a single-layer structure has been presented in [16,17]. The single-layer actuator consists of a narrower ‘‘hot’’ arm and a wider ‘‘cold’’ arm. The different thermal expansion between the hot arm and the cold arm will lead to an in-plane displacement of the actuator. Thus, the in-plane motion of the actuator is mainly due to the geometry design of the structure instead of material property of thin film. In attempt to overcome the drawback inherent in a multi-layer actuator, an out-of-plane electrothermal actuator of single-layer

☆ This paper was presented at the 15th IEEE MEMS conference, held in Las Vegas, USA, January 20–24, 2002, and is an expansion of the abstract as printed in the Technical Digest of this meeting.

* Corresponding author. Tel.: +886-3-574-2923; fax: +886-3-573-9372.
E-mail address: fang@pme.nthu.edu.tw (W. Fang).

0924-4247/03/$ – see front matter © 2003 Elsevier Science B.V. All rights reserved.
PII: S0924-4247(02)00315-1

structure is presented in [18]. This single-layer out-of-plane actuator also consists of a narrower "hot" arm and two wider "cold" arms. The different thermal expansion between the hot and the cold arms will lead to an out-of-plane displacement of the actuator. In this design, the performance and reliability of the actuator is limited to the thinner hot beam. A novel single-layer out-of-plane electrothermal actuator is investigated in this study. Since this actuator is consisted of only single-layer thin film material, it can prevent from delamination. Moreover, the structure is designed to allow bending upwards as well as downwards in the out-of-plane direction. Hence, this actuator can be driven in two directions, unlike the existing thermal actuators. The performance and reliability of the presented design was demonstrated in light of finite element analysis and experimental results.

2. Design and analysis

The presented actuator comprises four parallel, identical beams, as illustrated in Fig. 1a. These four beams are connected with a connecting arm at their free ends and then formed a single-layer thermal actuator. Since the inner beams and the outer ones are located at different planes, there are two steps at the free ends of the former ones. When a current only flows through the inner beams, they would experience a higher temperature rise as well as a larger thermal expansion. The beams are not coplanar, a larger thermal expansion on the inner beams would give rise to a torque, so as to induce an upward out-of-plane motion. On the contrary, while a current only flows through the outer beams, the actuator would experience a downward out-of-plane motion. The bi-directional out-of-plane motion is thus achieved. Since this actuator is consisted of only single-layer thin film material, the delamination problem in [19] can be prevented. In addition, the beams of the actuator have identical width, the disadvantage caused by the localization of higher temperature at the thinner beam in [18] can also be prevented.

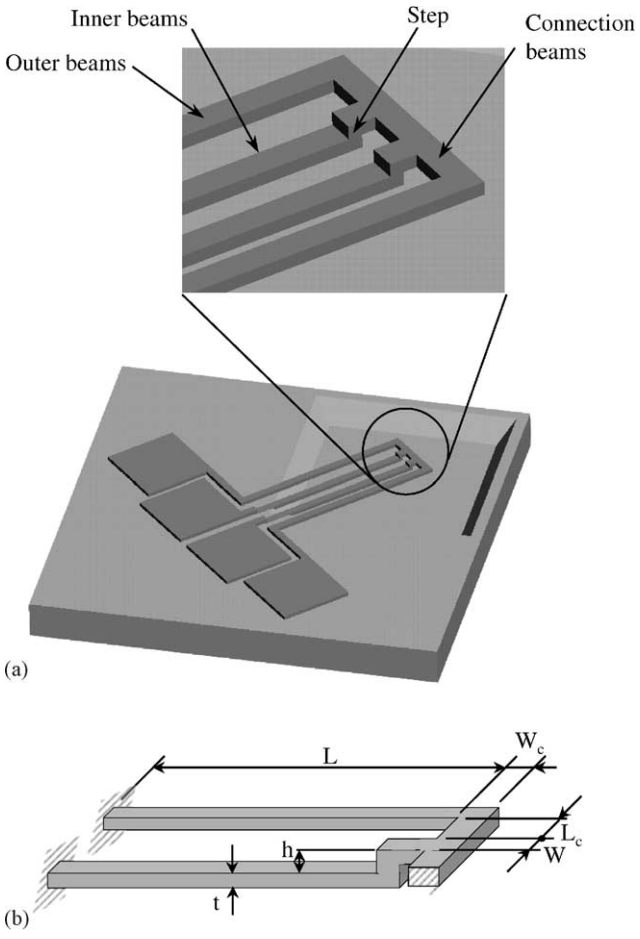

Fig. 1. (a) The schematic drawing of the single-layer electrothermal actuator and (b) the critical dimensions of the actuator.

The design was examined using commercial finite element software. In order to compare with the experimental results, the thin film material and substrate employed in this model is single crystal silicon. The material properties used in the FEM model are as follows, Young's modulus $E = 169$ GPa, coefficient of thermal expansion CTE $= 2.5 \times 10^6$, thermal conductivity $K_p = 157$ W/m °C, specific heat $S = 702.24$ J/kg °C, and resistivity $\rho = 1.1 \times 10^{-5}$ Ω m. In addition, various critical dimensions of the actuator including length L, width W, and thickness t of the beams, length L_c and width W_c of the connecting arms, and height h of the step, are indicated in Fig. 1b. The bending of the thermal actuator caused by the applying voltage was discussed. In addition, the temperature distribution of the actuator during operation was also studied. Consequently, the characteristics of the thermal actuator can be predicted.

Fig. 2 shows the typical simulation results on a thermal actuator. In the simulation, the critical dimensions of the beams and connecting arms are as follows, $L = 240$ μm, $t = 2$ μm, $W = 10$ μm, $L_c = 10$ μm, $W_c = 10$ μm, and $h = 2$ μm. Moreover, the actuator was applied with 5 V driving voltage at its inner beams. A typical simulation results regarding the temperature distribution of an actuator is shown in Fig. 2a. The temperature is distributed between 200 and 1300 K. As indicated in Fig. 2b, the temperature distribution of the inner beams and outer beams are depicted quantitatively. Since there is no current pass through the outer beams, they will only conduct the heat generated by the inner beams to the substrate. Thus, the temperature of the outer beams is decreased linearly from their tip to the ends. Since there is heat conduction from the connecting arm to the outer beams, the highest temperature of the actuator in this case will not occur at the tip of the inner beams. In general, the highest temperature region of the actuator is about a quarter away from the tip of the driving beams, according to the simulation. The simulation results regarding the deflection of an actuator are also discussed. The actuator was also applied with 5 V driving voltage at its inner beams during simulation. As shown in Fig. 2c, the

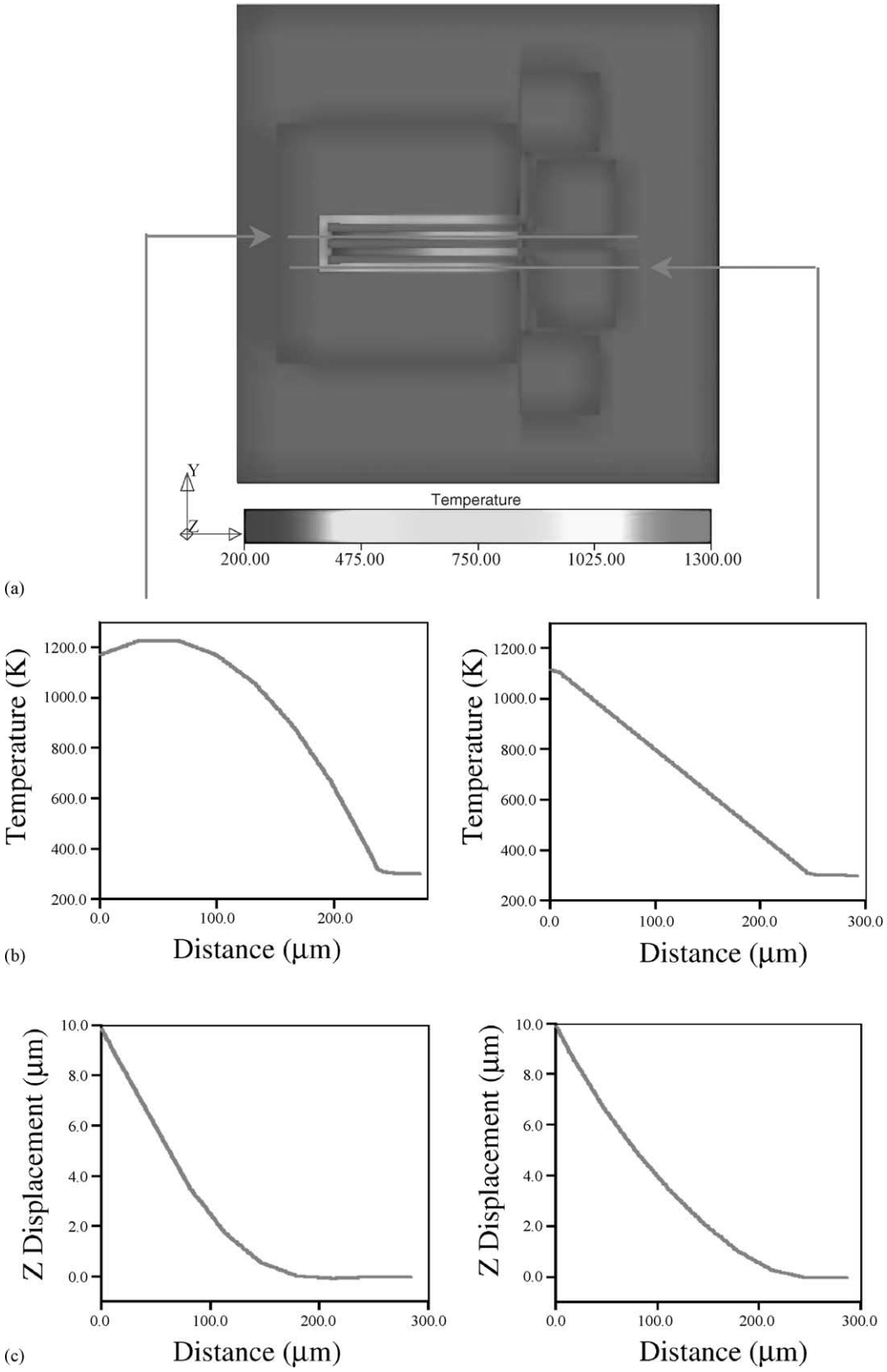

Fig. 2. The typical simulation results on a thermal actuator: (a) temperature distribution of the whole device, (b) temperature distribution along the inner and outer beams and (c) deflection profile of the inner and outer beams.

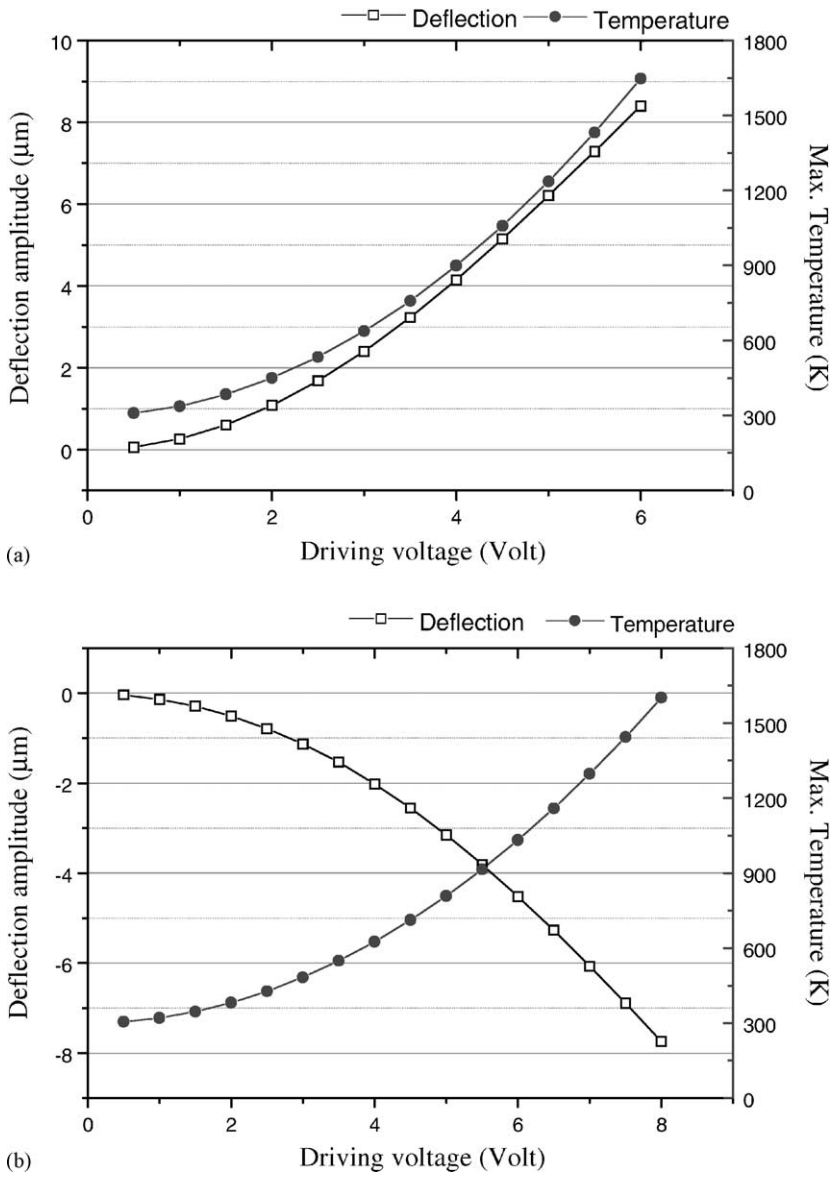

Fig. 3. Simulated maximum temperature and the deflection amplitude Δ versus the driving voltage when the actuator is moving (a) upwards and (b) downwards.

deflection amplitude at the tip of the actuator is near 10 μm upwards.

The simulated maximum temperature and the deflection amplitude Δ (i.e. tip deflection) of the actuator versus the driving voltage for the above case are also available in Fig. 3. The square dots in Fig. 3 show the variation of the deflection amplitude Δ of the actuator with the driving voltage. The circular dots in Fig. 3 show the maximum temperature of the actuator associated with the driving voltage when the ambient temperature is 298 K. The results in Fig. 3a reveal that the tip deflection of the actuator is 8 μm upwards when driven with 6 V at the inner beams. In this case, the maximum temperature of the actuator will reach 1650 K under 6 V driving voltage. On the other hand, the results in Fig. 3b reveal that the tip deflection of the actuator is 8 μm downwards when driven with 8 V at the outer beams. The maximum temperature of the actuator will reach 1600 K under 8 V driving voltage. According to the simulation results, it requires a larger driving voltage to bend the actuator downwards. This is mainly due to the difference of net resistance and thermal conductivity between the inner beams and the outer ones.

3. Experiment and results

In order to demonstrate the concept proposed in this study, the actuators were fabricated and tested. The fabrication processes that contain three masks are illustrated in Fig. 4. As shown in Fig. 4a, the silicon substrate was etched first to define the height h of the step. Heavily doped boron was exploited to define the structure of the actuator, as indicated in Fig. 4b and c. The silicon substrate bulk etching was

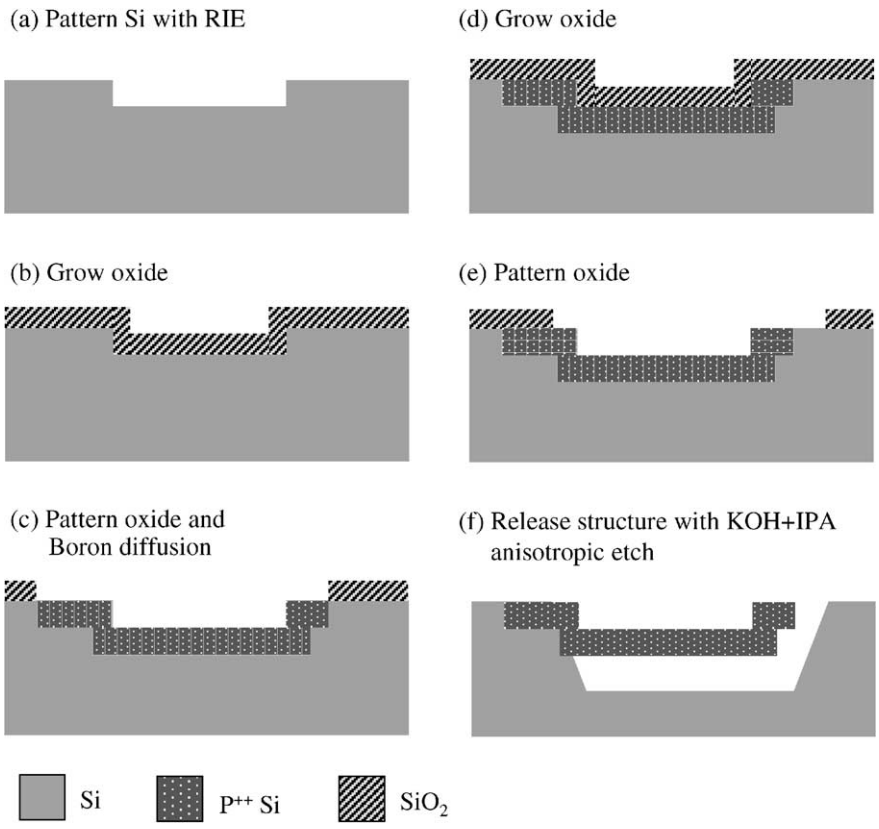

Fig. 4. Fabrication processes of the proposed electrothermal actuator.

conducted to release the actuator after the thermal oxide etching mask was patterned, as shown in Fig. 4d–f. Consequently, the actuator was formed by the single-layer boron doped silicon.

The test apparatus are illustrated in Fig. 5. To compare with the analytical results, the test was mainly focused on a 240 μm long, 10 μm wide, and 1.2 μm thick actuator. Firstly, the static deformation of the microactuator was measured. The actuator was driven by a DC signal from power supply, and the out-of-plane deformation of the beams can be measured by a non-contact optical interferometer. Two typical results measured when the actuator was driven

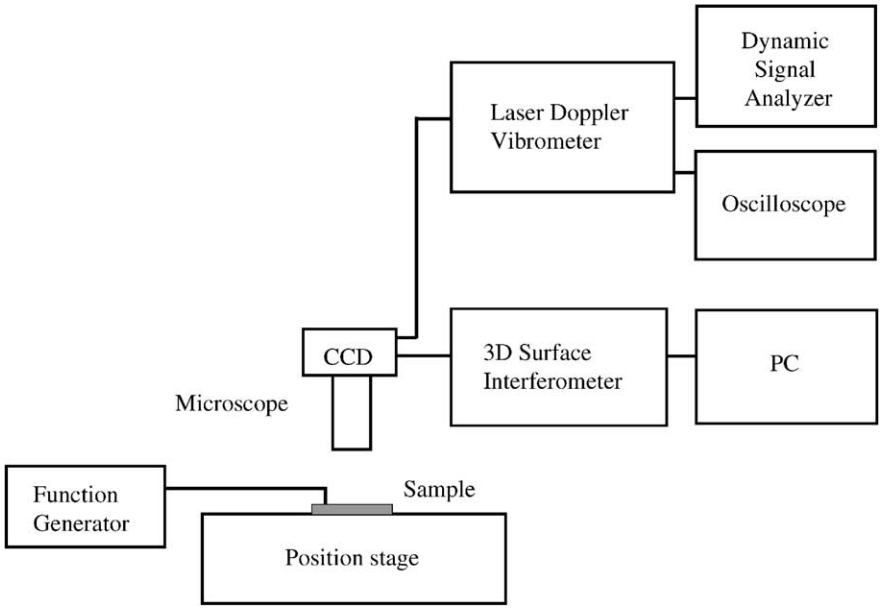

Fig. 5. The test setup for the electrothermal actuator.

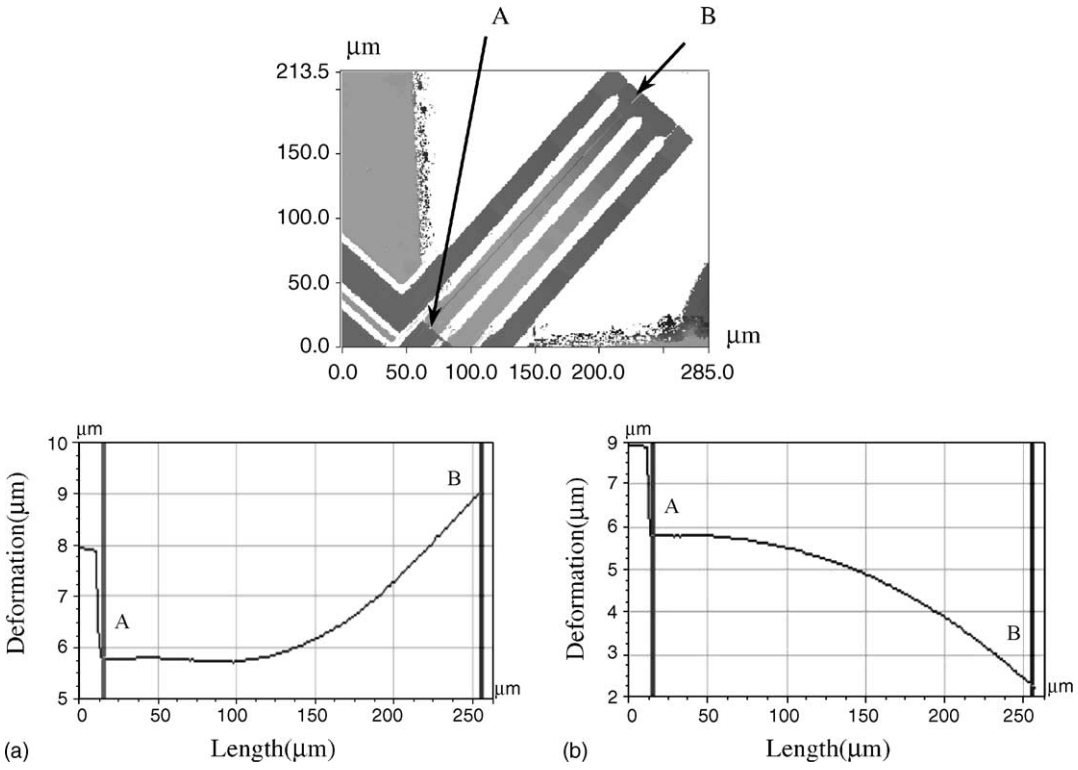

Fig. 6. Typical measured profiles of the actuator when it deflected (a) upwards and (b) downwards.

upward and downward are shown in Fig. 6. It demonstrates that the thermal actuator can be operated bi-directionally. As shown in Fig. 7, the variation of the deflection of the actuator with the driving voltage is determined. It shows that the actuator has an upward deflection amplitude Δ near 7 μm when driven at 5 V, however, the downward deflection amplitude Δ drops to 6 μm at the same driving voltage. Moreover, the highest temperature region can be qualitatively observed using CCD camera, as shown in Fig. 8. These photos show an actuator operating at 6.5, 6.7, and 6.85 V, respectively. The brightest region in the photos indicates the area with the highest temperature. It is obtained that the highest temperature region predicted by the simulation in Fig. 2 agrees well with the observation from CCD camera.

The dynamic response of the microactuator was also measured. In this case, the actuator was driven by an AC signal from function generator, and the out-of-plane velocity of the actuator can be measured by the laser Doppler vibrometer (LDV). The frequency response of the actuator is shown in Fig. 9a. It shows that the actuator has two peaks on its frequency response. As indicated in Fig. 9a, the first peak 1.89 kHz has a very broad bandwidth, and locates at lower frequency region. The second peak 35.8 kHz has a narrow bandwidth, and locates at higher frequency region. A vibration test was also conducted using a piezoelectric shaker [20]. In this experiment, the actuator was driven by an external shaker instead of the input AC. The measured frequency response in Fig. 9b shows the dynamic characteristics of the structure of the actuator. Apparently, the first natural frequency of the actuator is at 36.2 kHz. The vibration test demonstrates that the second peak in Fig. 9a corresponds with the natural frequency of the actuator. Consequently, the first peak of the frequency response is due to the thermal characteristic of the actuator. According to the measurement results, the actuator still has 2.2 μm out-of-plane deflection amplitude even when operation with a 2 V (peak-to-peak voltage), and 35.8 kHz sinusoidal wave signal.

The fatigue test was also conducted in this experiment. In this test, the thermal actuator was applying with 2.25 V and 32.9 kHz sinusoidal voltage. Typical fatigue test results are available in Fig. 10. As shown in Fig. 10a, the resonant frequency of the actuator has only 0.3% deviation after 10^9 cycles continuous operation. As shown in Fig. 10b, the vibration amplitude of the actuator remains at 2.36 μm for 10^7 cycles continuous operation. The vibration amplitude becomes unstable and will drop to 2.06 μm for 10^8 cycles continuous operation, after that it will increase to 2.34 μm for 10^9 cycles continuous operation.

4. Discussion and conclusion

A novel single-layer out-of-plane electrothermal actuator is designed and fabricated in this study. The thermal actuator is fabricated through the bulk micromachining processes. Unlike the bi-metal and hot–cold arm thermal actuator, this

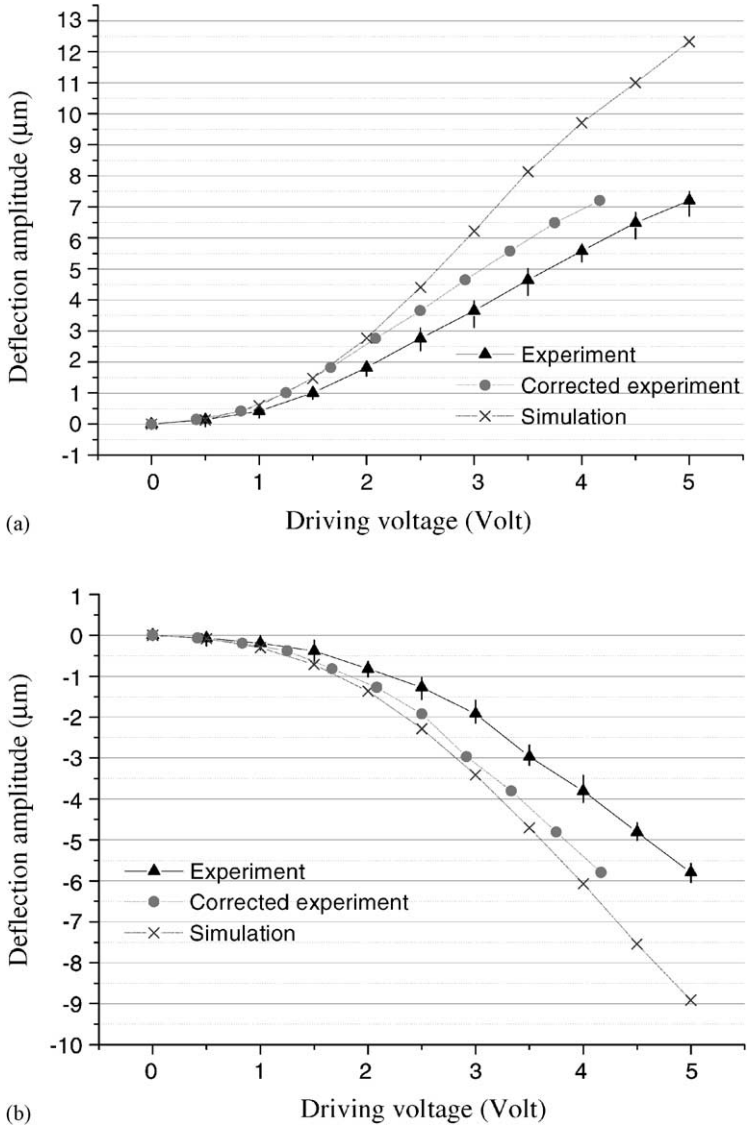

Fig. 7. The variation of the deflection amplitude Δ with the driving voltage when the actuator driven (a) upwards and (b) downwards.

actuator can move in two directions. The load–deflection test demonstrates that this actuator can achieve bi-directional actuation with amplitude near 6–7 μm when driven at 5 V. This characteristic enables the thermal actuator to perform as a bi-directional positioner. The vibration test shows that the thermal actuator still has a significant output when driven near 40 kHz. This characteristic enables the thermal actuator to perform as a resonant actuator. Since the proposed thermal actuator consists of only single-layer thin film material, it can prevent from delamination and its lifetime is significantly improved. The actuator were experienced a fatigue test which shows that its resonant frequency remains unchanged after 10^9 cycles of continuous operation with driving voltage at 2.25 V.

The variation of the driving voltage with the deflection amplitude Δ of the actuator is shown in Fig. 7, so as to compare the measured results with the simulation ones. It is obtained that the trend of the simulation results is similar to that of the measured ones. However, they still have a maximum 20% deviation in magnitude. The primary error source comes from the contact resistance between the probe tip and the bonding pad during experiment. Thus the measured displacement is smaller than the predicted one, as shown in Fig. 7. The problem can be improved by using the wire bond instead of the probe tip during experiment. Moreover, the ignorance of the thermal conduction due to air and the variation of material properties due to temperature change in the simulation model are also possible error sources. This problem can be improved by adding the air effect and by considering the variation of material properties to the simulation model.

As discussed in Section 3, the first peak in Fig. 9a is due to the thermal characteristic, and the second peak is resulted from the resonance of the structure. According to the measurement, the response of the actuator was dominated by its thermal characteristic in most of the frequency range.

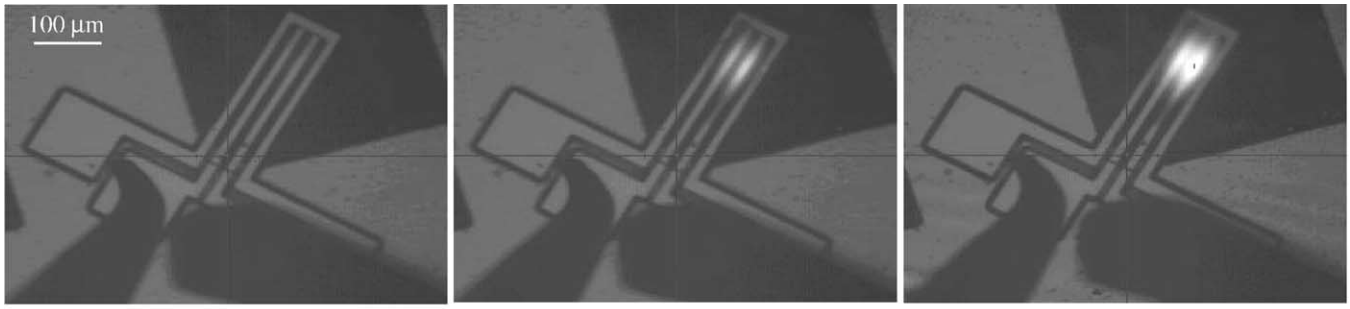

Fig. 8. The photos take from a CCD camera to show the highest temperature region on the actuator when the driving voltage is (a) 6.5 V, (b) 6.7 V and (c) 6.85 V.

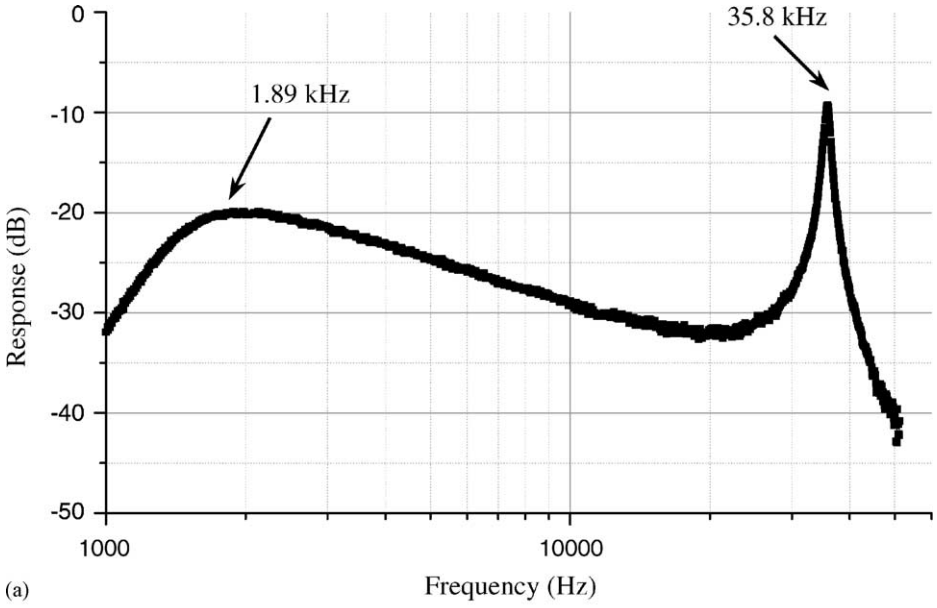

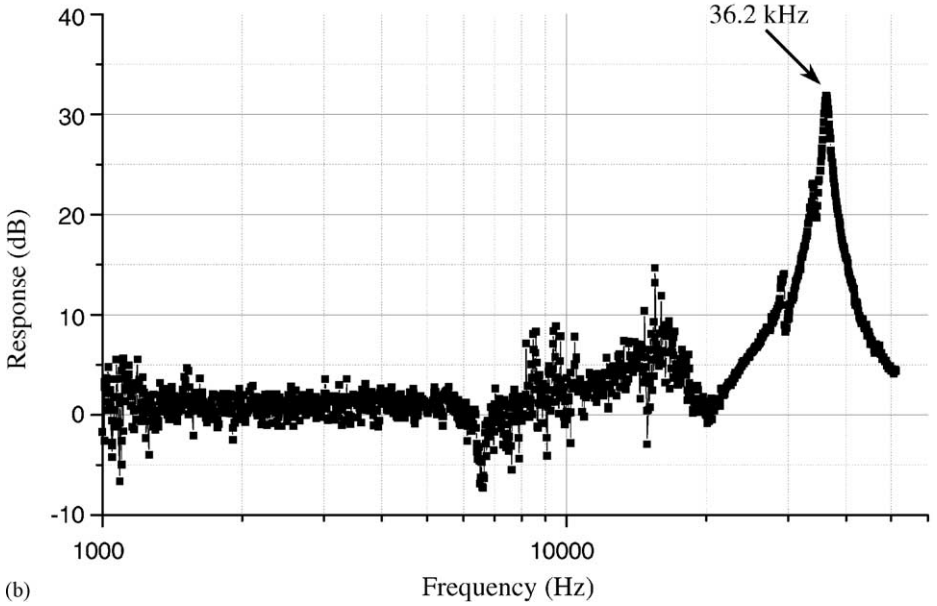

Fig. 9. The frequency response of the actuator when it is driven by (a) electrothermal approach and (b) external piezoelectric shaker approach.

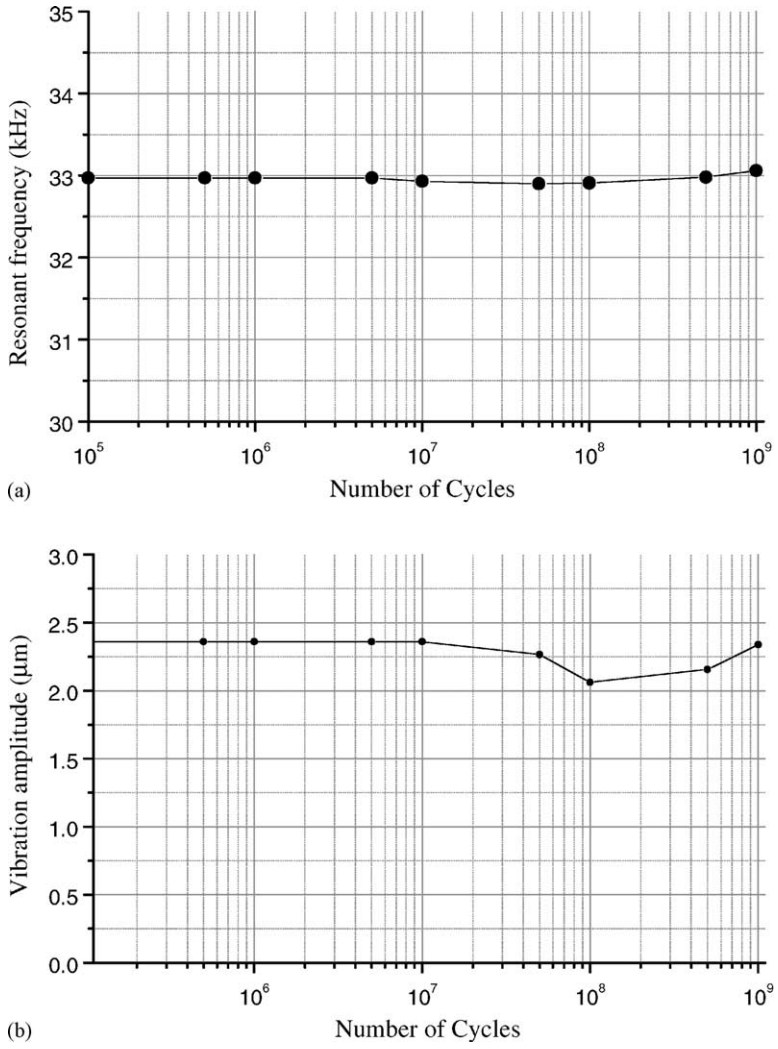

Fig. 10. Typical fatigue test results of the actuator, variation of (a) resonant frequency and (b) vibration amplitude with the test cycles.

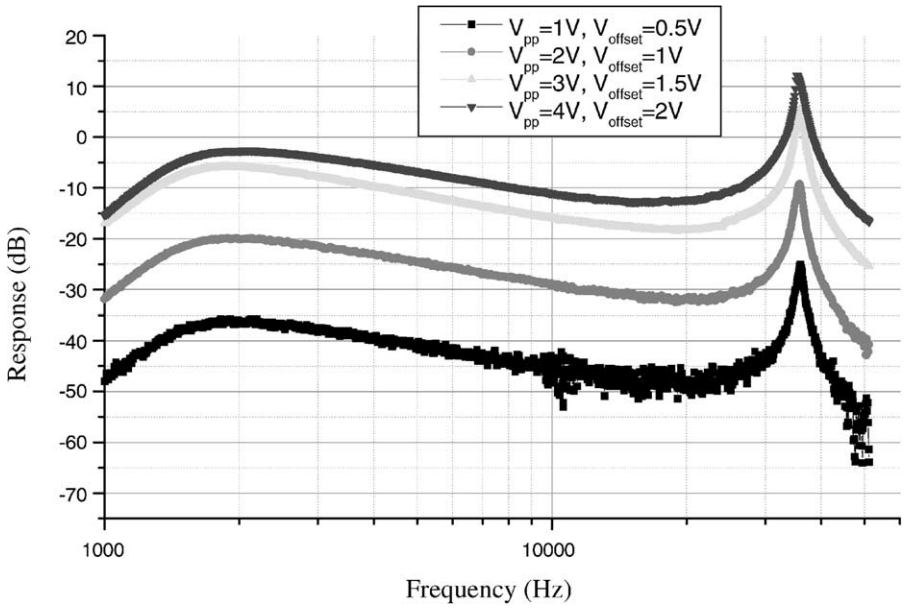

Fig. 11. The frequency response of the actuator when the driving voltage ranges from 1 to 4 V.

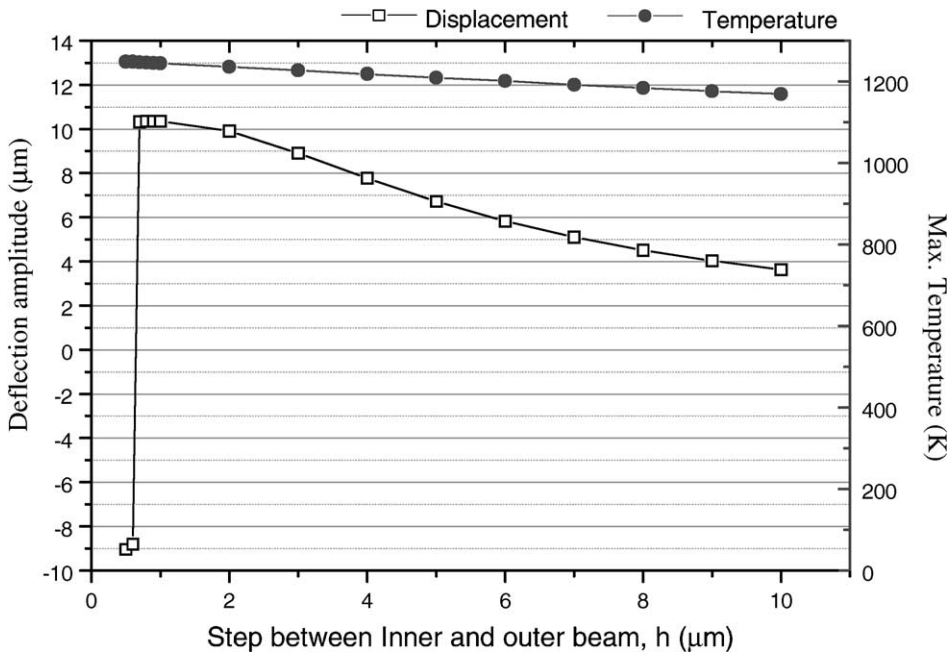

Fig. 12. Variation of the step height h with the deflection amplitude Δ of the actuator.

Hence, the response of the actuator is gradually increased until it reaches the first peak, and then gradually decreased. The response of the actuator was dominated by its vibration mode only at a small frequency range. In this region, the response is increased and decreased drastically. Fig. 11 shows the frequency response of the actuator when the applying voltage ranging from 1 to 4 V. The first peak near 1.9 kHz that corresponds to the thermal characteristic of the actuator was slightly decreased when the driving voltage was increased. This is caused by the temperature change of the actuator for different driving voltages. However, the second peak that corresponds to the structural dynamics of the actuator remains at 32.9 kHz for different driving voltages. The resonant frequency of the actuator is more stable during the variation of the temperature. In short, the thermal actuator can be exploited as a resonant actuator with a large output at high frequency. The operating frequency of the resonant actuator can be easily adjusted by changing the dimensions of the beams.

The performance of the thermal actuator can be optimized by changing the dimensions of beams, connecting arms, and step height. The most critical dimension to influence the performance of the thermal actuator is the step height h. The variation of the step height h with the deflection amplitude Δ of the actuator was investigated through the simulation means, as shown in Fig. 12. When the height h is increased, the stiffness of the step is decreased. The thermal expansion of the driving beams could be relaxed through the deflection of the step. Consequently, the displacement of the actuator is decreased. On the other hand, the stiffness of the step is increased when the height h is decreased. Thus the bending moment caused by the thermal expansion of the driving beams is decreased since the moment arm is decreased. Moreover, the driving beams may buckle instead of bending to relax the thermal expansion. In this regard, the displacement of the actuator could be either upward or downward. As shown in Fig. 12, it is difficult to predict the tip displacement Δ of the thermal actuator when its step height is smaller than 1 μm.

Acknowledgements

This paper is based (in part) upon work supported by the National Science Council (Taiwan, ROC) under Grant NSC 89-2218-E007-042. The author would like to express his appreciation to the NSC Central Regional MEMS Research Center (Taiwan, ROC), Electrical Engineering Department of National Tsing Hua University (Taiwan, ROC), Semiconductor Center of National Chiao Tung University (Taiwan, ROC), and National Nano Device Laboratories (Taiwan, ROC) in providing fabrication facilities.

References

[1] L.S. Fan, Y.C. Tai, R.S. Muller, Integrated movable micromechanical structures for sensors and actuators, IEEE Trans. Electron Dev. ED-35 (6) (1988) 724–730.
[2] W.C. Tang, T.H. Nguyen, R.T. Howe, Laterally driven polysilicon resonant microstructures, Sensor Actuator A 20 (1989) 25–32.
[3] T. Akiyama, K. Shono, Controlled stepwise motion in polysilicon microstructures, J. Microelectromech. Syst. 2 (3) (1993) 106–110.
[4] H. Matoba, T. Ishikawa, C.-J. Kim, R.S. Muller, A bistable snapping microactuator, in: Proceedings of the IEEE Micro Electro Mechanical Systems Workshop, Oiso, Japan, January 1994, pp. 45–50.
[5] C. Liu, T. Tsao, Y.C. Tai, Out of plane permalloy magnetic actuators for delta-wing control, in: Proceedings of the IEEE Micro Electro

Mechanical Systems Workshop, Amsterdam, Netherlands, January 1995, pp. 7–12.
[6] J. Hsieh, W. Fang, A novel micro electrostatic torsional actuator, Sensor Actuator A 79 (2000) 64–70.
[7] H. Schenk, P. Dürr, D. Kunze, H. Lakner, H. Kück, A resonantly excited 2D-micro-scanning-mirror with large deflection, Sensor Actuator A 89 (2001) 104–111.
[8] R. Chen, H. Nguyen, M. Wu, A low voltage micromachined optical switch by stress-induced bending, in: Proceedings of the IEEE Micro Electro Mechanical Systems Workshop, Orlando, FL, January 1999, pp. 424–428.
[9] M. Sakata, Y. Komura, T. Seki, K. Kobayashi, K. Sano, S. Horiike, Micromachined relay which utilizes single crystal silicon electrostatic actuator, in: Proceedings of the IEEE Micro Electro Mechanical Systems Workshop, Orlando, FL, January 1999, pp. 21–24.
[10] D.J. Young, B.E. Boser, A micromachined variable capacitor for monolithic low-noise VCOs, in: Proceedings of the IEEE Solid-State Sensor and Actuator Workshop, Hilton Head Island, SC, June 1996, pp. 86–89.
[11] T. Seki, M. Sakata, T. Nakajima, M. Matsumoto, Thermal buckling actuator for micro relays, in: Proceedings of the 1997 International Conference on Solid-State Sensors and Actuators (Transducer'97), Dig. Tech. Papers, Chicago, IL, June 1997, pp. 1153–1156.
[12] X.-Q. Sun, K.R. Farmer, W.N. Carr, A bistable microrelay based on two-segment multimorph cantilever actuators, in: Proceedings of the IEEE MEMS'98, Heidelberg, Germany, January 1998, pp. 154–159.
[13] S. Schweizer, S. Calmes, M. Laudon, P. Remaud, Thermal actuated optical microscanner with large angle and low consumption, Sensor Actuator A 76 (1999) 470–477.
[14] W. Benecke, W. Riethmuller, Applications of silicon-microactuators based on bimorph structures, in: Proceedings of the IEEE MEMS'89 Workshop, Salt Lake City, UT, February 1989, pp. 116–120.
[15] J.R. Reid, V.M. Bright, J.H. Comtois, Automated assembly of flip-up micromirrors, in: Proceedings of the 1997 International Conference on Solid-State Sensors and Actuators (Transducer'97), Dig. Tech. Papers, Chicago, IL, June 1997, pp. 347–350.
[16] J.H. Comtois, V.M. Bright, Applications for surface-micromachined polysilicon thermal actuators and arrays, Sensor Actuator A 58 (1997) 19–25.
[17] D.M. Burn, V.M. Bright, Design and performance of a double hot arm polysilicon thermal actuator, in: Proceedings of the SPIE Micromachining and Microfabrication Conference, Austin, TX, September 1997, pp. 296–306.
[18] C. Lo, H.-Y. Lin, W. Fang, A novel out-of-plane electrothermal microactuator, in: Proceedings of the 2001 Microsystem Technical Conference, Dusseldorf, Germany, March 2001.
[19] S.B. Brown, E. Jansen, Reliability and long term stability of MEMS, in: Proceedings of the IEEE/LEOS 1996 Summer Topical Meeting, Keystone, CO, August 1996, pp. 9–10.
[20] H.-C. Tsai, W.P. Lai, W. Fang, Characterizing the Poisson's ratio of thin film using resonance method, in: Proceedings of the 2001 ASME International Mechanical Engineering Congress and Exhibition (IMECE), No. 23851, New York, NY, November 2001.